ASPS Conference Proceedings 1: 1429-1439 (2022)

Proceedings of

12th Structural Engineering Convention-An International Event (SEC 2022)

Available at https://asps-journals.com/index.php/acp

Application of UPV-Instrument in Health Monitoring of Indian Rail Section Using AE Technique

Tamal Kundu[1,*], Apurba Pal[1], Parikshit Roy[1], Aloke Kumar Datta[2] and PijushTopdar[2]

[1] Research Scholar, National Institute of Technology Durgapur, West Bengal, India
[2]Associate Professor, National Institute of Technology Durgapur, West Bengal, India

Paper ID - 130308

Abstract

The health monitoring of rail sections from the perspective of safety is a significant field of research in the context of the Indian Railways, which is thought to be Asia's second-largest rail network. The main focus of health monitoring is to assess damages and determine their location in order to initiate the appropriate measures. One of the well-known Non-Destructive Techniques (NDTs), Acoustic Emission (AE) technique can be used for this purpose. However, the literature suggests that the appropriate localization of damage, which is in fact an AE source, is challenging due to the complex geometry of the rail section. Continuous research going on in this direction and the pencil lead break (PLB) method often serves the purpose of simulated AE source in the experimental investigation of these research works. There are a few limitations present in the PLB method due to its manual operation. In the practical scenario, PLB requires expertise to operate perfectly. Moreover, the complexity of the application of PLB is increased in case of uneven surfaces. In this context, PLB can be replaced by an Ultrasonic Pulse Velocity (UPV) instrument. UPV instrument produces an ultrasonic signal which is very similar to PLB. In this study, an effort is paid to detect and localize the simulated AE sources produced by a UPV instrument in the Indian rail section under laboratory conditions using AE technique. Earlier researchers used Wavelet Transform (WT)-based localization to calculate distance between AE source to placed sensor on the material. It is observed from the WT-based localization of AE sources that in rail section WT-based localization can be valid up to a certain distance due to complex geometry of the rail section. But with the WT of the obtain AE signal induced from PLB and UPV over the rail section is compared. It is observed that the UPV and PLB produces similar signal. In this paper, the localisation of such simulated AE sources is done using an Artificial Neural Network (ANN) based methodology. The ANN model is developed using the basic parameters of the AE signal. Further, a set of PLB sources are also applied to the rail section and localization of these sources is also done. Localisation results of both simulated AE sources, PLBs and UPV-generate dones, are compared. It is found that the localization using ANN of the simulated AE source is done with a minimal error of 1.3%. The technique is promising and there is a good scope for future research and application in health monitoring of different types of structures.

Keywords: Acoustic Emission, Rail Section, NDT, Simulated AE Signal, UPV Instrument, Indian Railway, ANN, SHM

1. Introduction

In many countries around the world, including India, railways play a significant role in transportation. Indian Railways –the lifeline of the nation - has recently incurred financial losses and fatalities due to a number of derailments, most of which were brought on by rail iron track breakdown. Heavy traffic and exposure to the environment may cause the rail iron track to deteriorate. Rigorous monitoring of these rail sections using the Non-Destructive Technique (NDT) is necessary to reduce the maintenance cost and evaluate the condition. Damage localization is one of the main concerns when it comes to monitoring the condition of a structure [1]. However, there are a number of conventional NDTs available to identify and localise damage. Among those, Acoustic Emission (AE) is one of the popular NDTs and is adopted by many researchers to develop a Structural Health Monitoring (SHM) system for significant influence on public safety, performance and extending the life of ageing structures. Moreover, real-time localization with accuracy can be done using the same methodology [2]. AE method, which is a passive technique, uses elastic stress waves that are released rapidly when a crack initiates and grows. Analysing AE signals, recorded by employing AE sensors or transducers over the specimen, structural damage or AE source can be localized [3]. Using this method damage can be localized in real-time for rail sections without violating the traffic if a sudden failure occurs [4].

*Corresponding author. Tel: +91-9733118555; E-mail address: tk.18ce1101@phd.nitadgp.ac.in

Published online: December 19, 2022
doi:10.38208/acp.v1.673

Since the AE technique is introduced, several researchers carried out studies towards enhancing the accuracy of damage localization. Due to the complex geometry of rail section, it is quite difficult to detect damage accurately. The different portions of the rail section (Top Flange, Web, and Bottom Flange) are considered as simple plates by several researchers for ease of computation [5]. Previously, damage/source localization in a plate-like structure using the elastic wave propagation rule of AE is examined by Hamstad (1999-2002) [6-8]. Also, Hamstad (2009) studied the effect of propagation from different distances and depths in a 25 mm thick steel plate [9]. Thereafter, the source localization approach using the AE technique has been employed for the diagnosis of the rail sections [10-11]. By installing an AE transducer on the rail top, Bassim (1994) demonstrated the AE technique's vast capabilities in identifying geometric faults on the smooth surface of the wheel periphery [12]. Through creating a test rig, Bruzelius and Mba (2004) conducted an experiment on the applicability of AE for identifying flaws and surface integrity of iron rail sections [13]. LiD et al. (2018) conducted rail crack monitoring in the field, with complex cracking conditions and operating noise, using Tsallis synchrosqueezed wavelet entropy using the AE approach [14].

Earlier researchers used signal processing techniques to localize simulated damages induced by pencil-lead-break (PLB) in the rail section in the laboratory environment. PLB is popularly used as a simulated AE source for its reproducibility. PLB is carried out by breaking pencil lead of specific hardness at a specific angle – generally 30° to 45° – with 3 to 4 mm free lead length. But there are a few limitations present in the PLB method due to its manual operation. In the practical scenario, PLB requires expertise to operate perfectly. Moreover, the complexity of the application of PLB increases in case of uneven surfaces. In this context, PLB can be replaced by an Ultrasonic Pulse Velocity (UPV) instrument since the UPV instrument produces an ultrasonic signal which is very similar to PLB. It is observed from the experiment that WT- based localization is valid up to a certain distance in the rail section. Due to the complex geometry of the rail section, the mode mixing and reflection arrive faster.

In this study, an effort is paid to detect and localize the simulated AE sources produced by a UPV instrument in the Indian rail section under laboratory conditions using the AE technique. The capability of the UPV instrument to emit signals of constant frequencies is used in this study to simulate the AE source. The testing is done at the top flange of the rail section. An AE sensor is fixed on the same surface and the AE signals are recorded at 50mm intervals. Further, the PLB source is also used at the same locations to capture AE signals. Localization of simulated AE sourcesis done using an ANN methodology. Thereafter,the localization results of the UPV instrument are compared with the localization results of PLB to check the efficacy of UPV induced AE source. It is found that the UPV instrumentis a better choice since it is comparatively error-free,as it is completely mechanically operated while PLB is done manually.

Methodology

This paper discusses the use and effectiveness of the UPV instrument, which can replace the conventional PLB approach and be used as an emitter of the ultrasonic signal.PLB and UPV are done to generate AE sources which are synonymous with the actual crack and are done on the top flange of the rail section which is in undamaged condition brought from Indian Railway in undamaged condition. The emitter probe of the UPV is mounted on the top flange of the rail section Also the PLB is done in the top flange. The induced AE signal by both PLB and UPV is captured using the AE sensor in a 50 mm interval. The obtained AE signal from different segments of the rail section is analysed with signal processing approach called Wavelet Transformation (WT). But it is observed that the AE source localisation with WT is difficult due to geometry of the rail section. In this paper, WT is done using a software AGU-Vallen. Localisation of the AE sources are done by superimposing group velocity curve over the WT diagram of the obtained AE signal. This group velocity curve is calculated with theoretical values of longitudinal and shear velocities i.e., 5.9 m/ms and 3.1 m/ms.The localisation of AE sources can be done up to a certain distance. But the fundamental parameters are the basic feature of a signal. Therefore, these parameters are used to localise the AE sources over the rail section. The localisation of the induced signal is done using ANN. ANN is a powerful tool that can predict the location of damage by analysing provided datasets for training. But with the WT technique comparison of the both signals are done. It is observed from the comparison that from PLB and UPV both case we are getting the accurate results. All the experiments are done in a 1.9 meters rail section of 60Kg/m.

The main focus of the paper is to replace PLB with UPV instrument. In this paper, AE source localization using ANN is done with the help of the fundamental features of the AE signal. The methodology is represented in a flowchart in **Fig. 1**. 3D representation of the WT diagram of the obtained AE signal due to PLB is shown in **Fig. 2**. Therefore, obtaining good quality signal is the main concern for this technique. These fundamental features of the AE signal are shown in **Fig. 3** (RMS, Duration, Energy, Peak Frequency, Amplitude) taken to train the ANN model. As these parameters has a influence on the AE signal from different depths and distances, in the developed ANN model different weight functions are allocated on the individual parameters of the obtained AE signal. For the convenience of the experiment, these features are separated into four clusters. These clusters are mentioned in **Table 1**. After that, the ANN model is prepared in MATLAB. The ANN model uses four hidden layers and twenty neurons consisting in each layer. **Fig. 4** depicts the ANN model developed in MATLAB. **Table 2** depicts the orientation of the data set for Input, Training, and testing purpose.

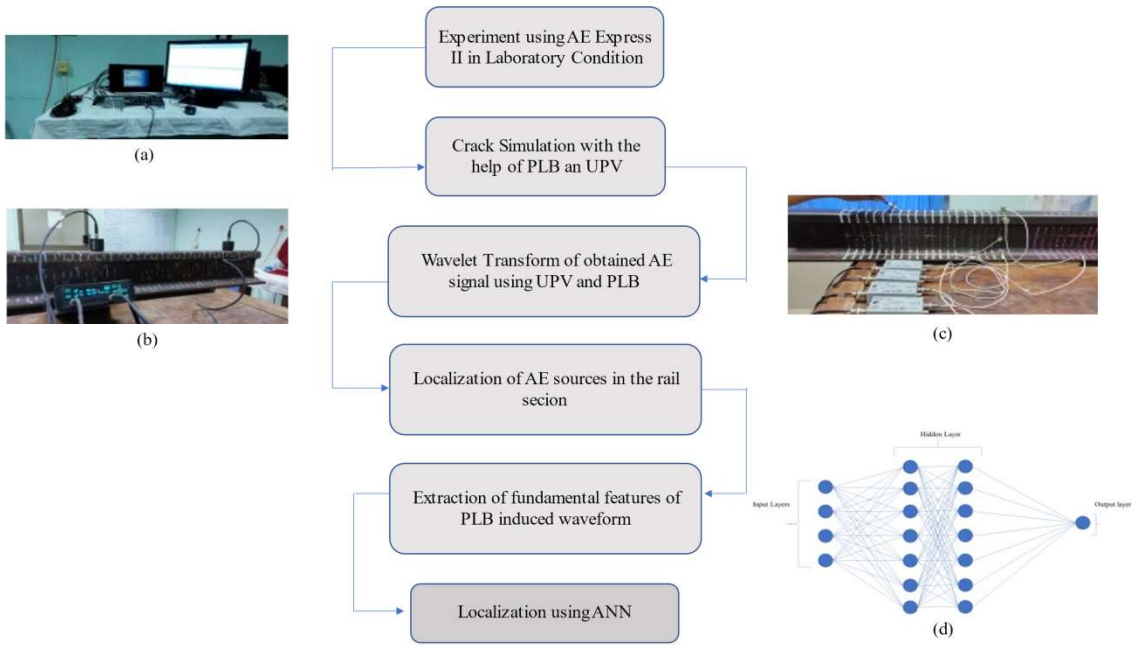

Fig. 1 Flowchart of the methodology: a) AE system, (b) UPV Emitter on Rail, (c) PLB on Rail, d) Representation diagram of the ANN model.

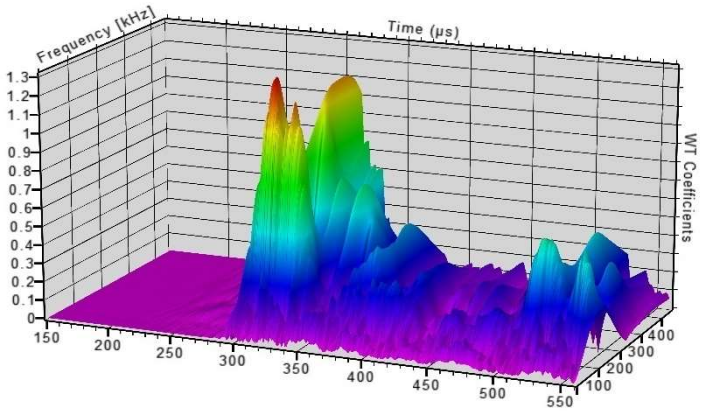

Fig. 2: A 3D representation of WT diagram of obtained AE signal due to PLB

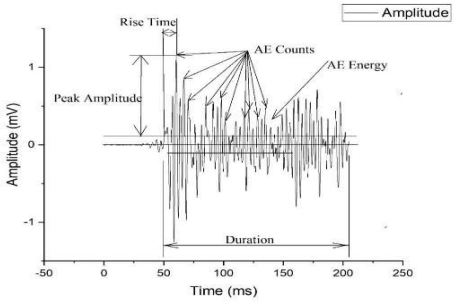

Fig. 3 Fundamental Features of AE Wave

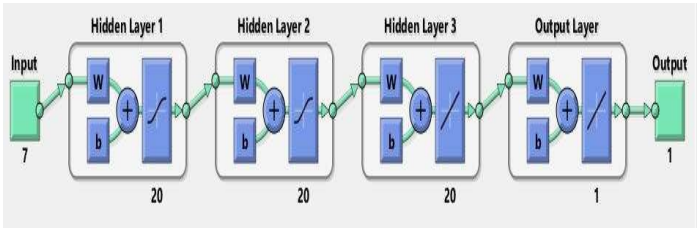

Fig. 4 Developed ANN Model

Table 1 Clusters Made for ANN

Cluster	Arrangements of Fundamental Properties of Signal
C1	Rise time, Energy, Amplitude, Peak Frequency
C2	Rise time, RMS, Energy, Duration
C3	Rise time, Duration, Counts, RMS
C4	RMS, Duration, Energy, Peak Frequency, Amplitude

Table 2. ANN Data Structure

ANN Cluster	Data Structure Input Size	Data Structure Training/Test Samples	Model Parameter Trainable
C1	1200X4	800/350	4800
C2	1200X4	800/350	4800
C3	1200X4	800/350	4800
C4	1200X4	800/350	4800

Experimental Setup

To localize the damage in the rail section with the above-discussed methodology the following setup is done. **Fig. 5** depicts the experimental setup for testing in the rail section. The experiment is carried out on a 1.9 m rail section provided by Indian Railways. The data acquisition system for AE monitoring is procured from Physical Acoustic Corporation (PAC). PLB is taken to simulate the AE source in the media. A differential type (WD) AE sensor or transducer, procured from PAC is utilized as a receiver to detect the simulated AE wave generated from various propagation distances. **Fig. 5 (b) and Fig. 6 (b)** is the representation of the placement of AE sensors on the rail section. Excitation with the PLB and UPV is done on the top flange of the rail section to simulate the AE signal. PLB is done with the 45^0angle and 3mm lead length.

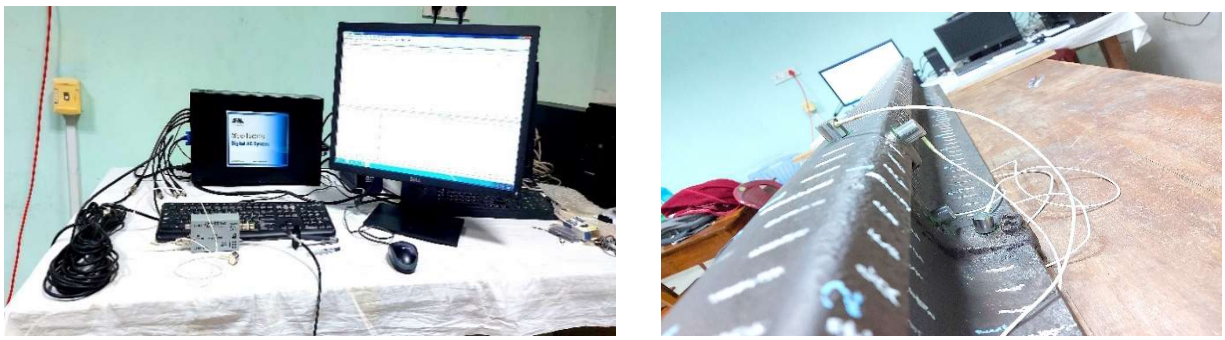

(a) **(b)**

Fig. 5: The experimental setup for rail testing, a) AE Instrument, b) Rail Section

Measurement positions on the top flange, web and bottom flange of the rail section are depicted in **Fig. 6 (a) and (b)**. For testing reasons, multiple measurement points in the above-mentioned region were considered. The AE receiver was mounted on flat places such as the top flange's head, the middle of the rail section's web, and the flat area of the bottom flange. The AE receiver is installed on a web that is 70 mm below the rail section's top flange. With 50 mm intervals, measurement positions have reached up to 1200mm.Acquiring a consistent and homogenous actual simulated acoustic source is fairly difficult. Though AE sensors can simulate a homogeneous and stable AE source, PLB has been used to obtain an accurate AE source with varying depths of rail section and propagation distances. The frequency of the PLB source is usually between 100 and 200 kHz. Therefore, an ultrasonic signal is produced by 150 kHz with the UPV instrument.

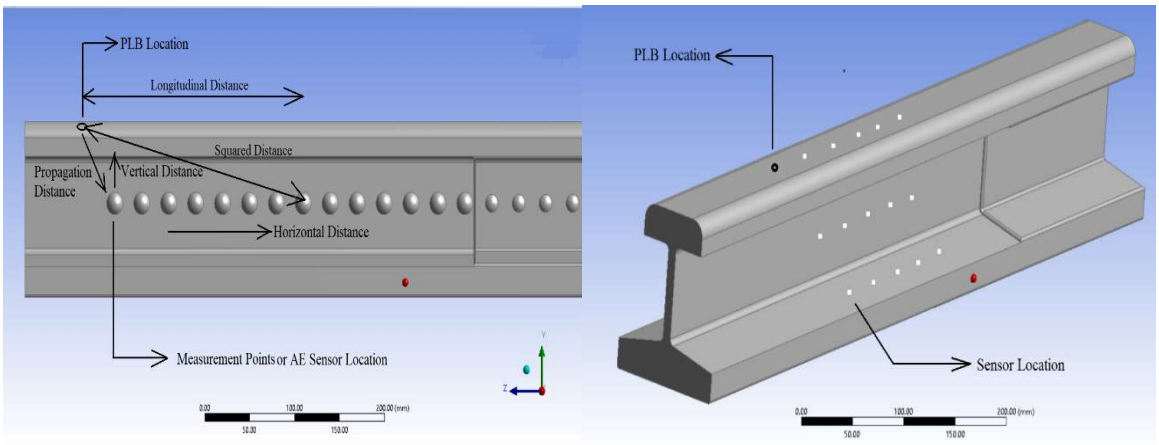

(a) (b)

Fig. 6: (a) Representation of the side view of the rail and measurement distances; (b) Placement of AE sensor location and PLB location

All of the data in this research was collected using the AE acquisition system (AE Win 8) at a sampling frequency of 1 MHz. All the data were evaluated during a time span of 0-1000 microseconds. Localisation is done with the help of a single sensor approach.

Experimental Studies

In this paper, UPV and PLB simulated AE sources are implemented on the Top Flange of the rail section. Impact using UPV and PLB both have done a particular position in the TF position of the rail section. Three AE sensor is placed on the TF (S1), Web (S2), and BF (S3) position of the rail section. AE sensor is placed on the same surface and AE burst is collected at 50mm intervals. **Fig. 7** depicts the comparison of acquired AE signals of S1, S2, and S3 induced by UPV. In **Fig. 8** PLB and UPV-induced AE signal patterns are compared with each other. It is clear from **Fig. 8** that both sources are comparable to other.

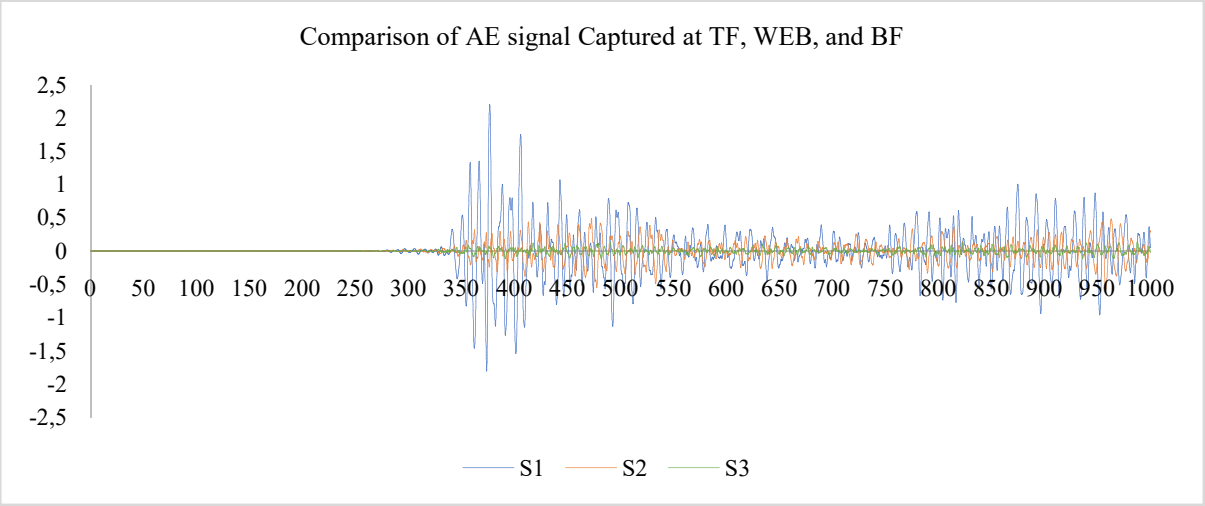

Fig. 7 Comparison of the AE Signal Acquired by S1, S2 and S3 Induced by PLB

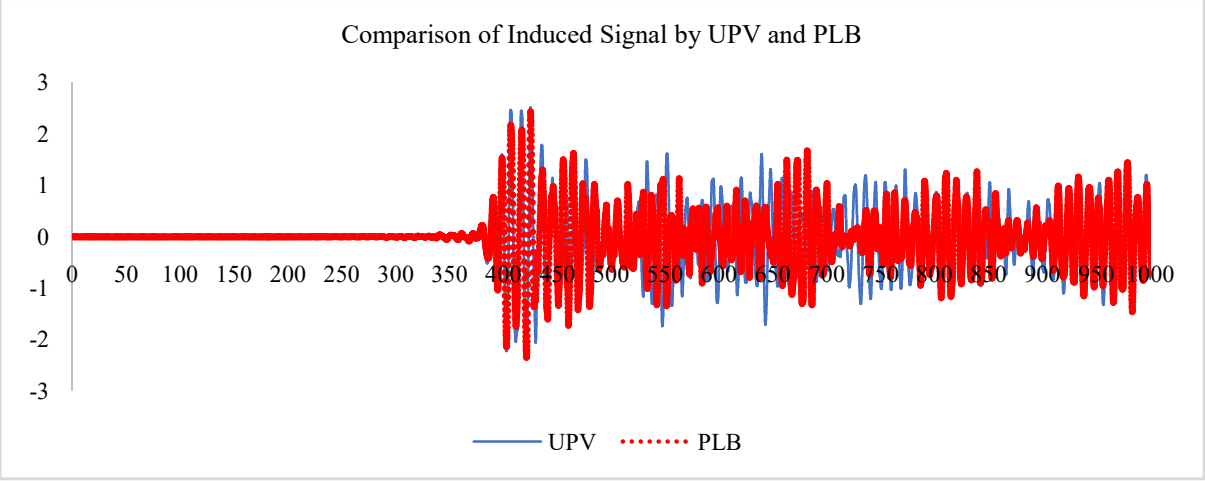

Fig. 8 Comparison of UPV and PLB Induced AE Signal at 500 mm Distance from the Source

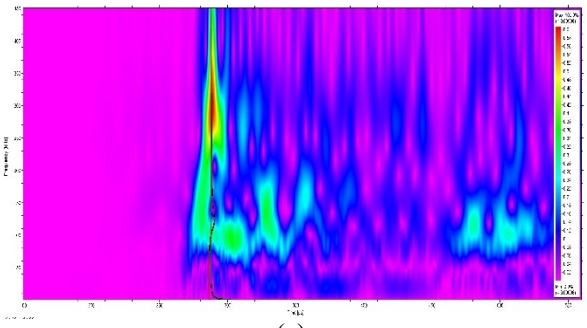

(a)

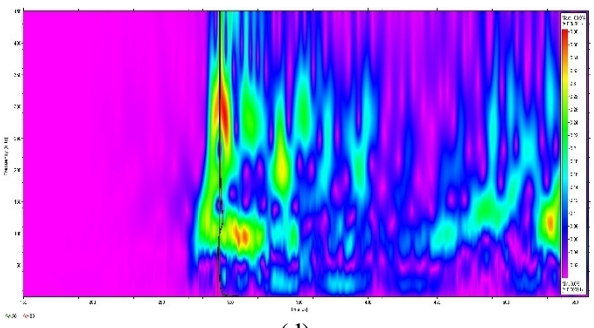

(d)

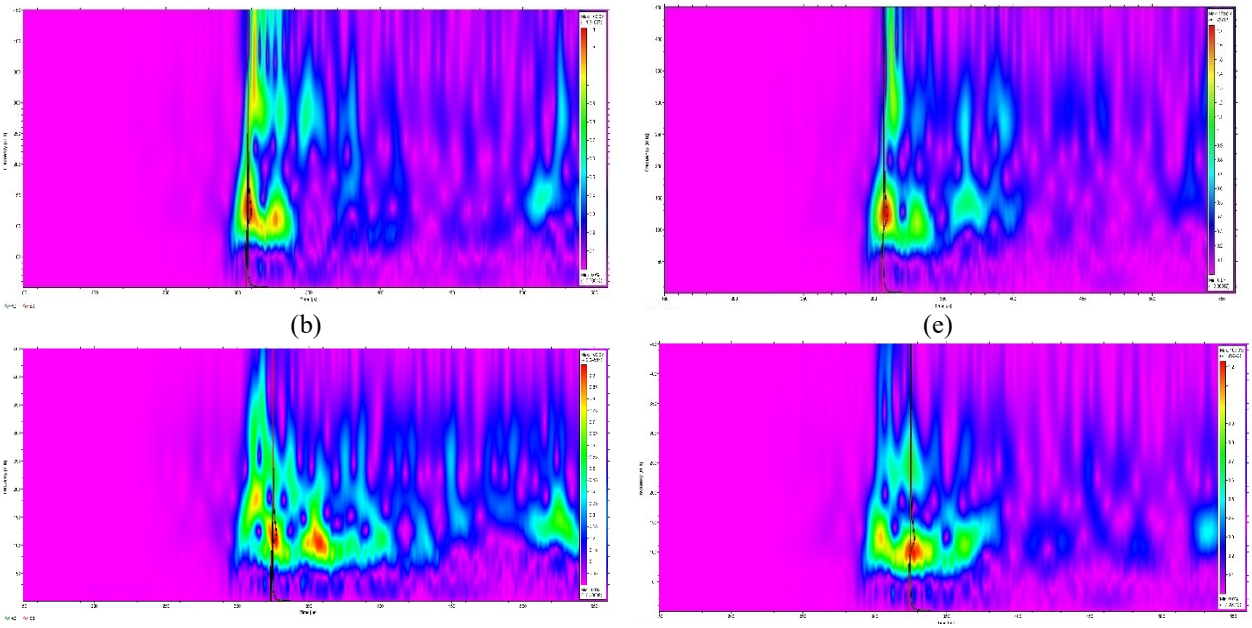

Fig. 9: (a), (b), (c) are the WT diagram of the obtained AE signal induced from PLB; (d), (e), (f) are the WT diagram of the obtained AE signal induced from UPV

The obtained AE signal from different segments of the rail section is analysed with signal processing approach called Wavelet Transformation (WT). But it is observed that the AE source localisation with WT is difficult due to geometry of the rail section. The localisation of AE sources can be done up to a certain distance that is 300mm. But the fundamental parameters are the basic feature of a signal. Therefore, these parameters are used to localise the AE sources over the rail section. Thereafter fundamental features of both signals are extracted for the localisation of the AE source using the ANN approach.

Result and Discussion

It is clear from the **Fig. 9** UPV can emit the similar AE signal is induced by PLB. The ANN model for the localisation of the induced AE source, has been prepared in MATLAB. Four clusters are prepared using the data-driven parameters in order to detect damage locations precisely. The model is prepared using different types of weight functions in the input layer. Weight functions are introduced in all four clusters to check the best performance of the developed ANN model. The performance of the developed ANN model is checked and validated using the trial-and-error method. From **Fig. 10** it is clear that cluster 4 can predict the appropriate result as the R-value is reached 1. The number of neurons used in the ANN's hidden layer has an influence on MSE and R. The R-value, which ranges from 0 to 1, reflects the relationship between output and targets. In this investigation, the model uses five input layers and four hidden layers and each hidden layer consists of twenty neurons. Mean Square Error (MSE) is used in the ANN model to get the output value as close as the target value. Feed Forward Back propagation is introduced in the model to achieve the target value. After training the model is stopped after 750 iterations. The ANN model runs for 15.5 minutes on average to complete each localisation process.

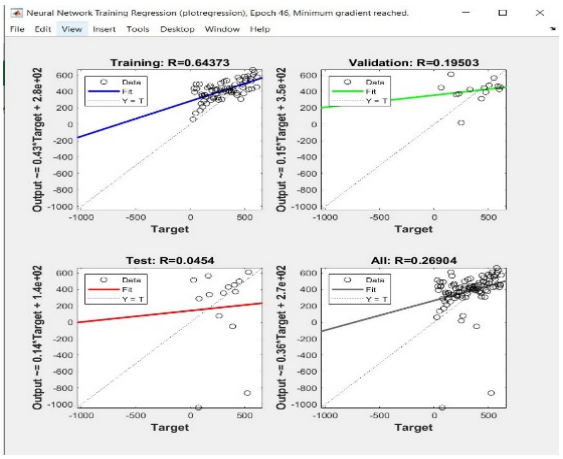

(a)

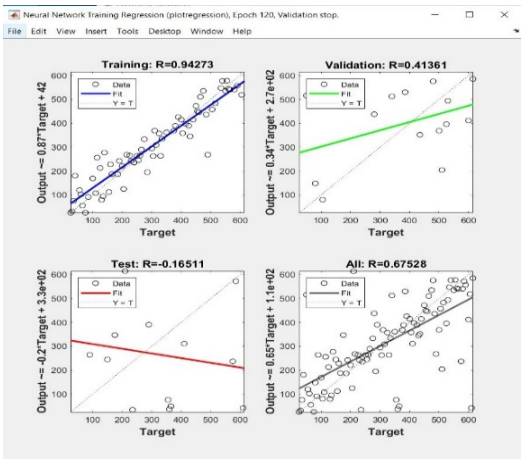

(b)

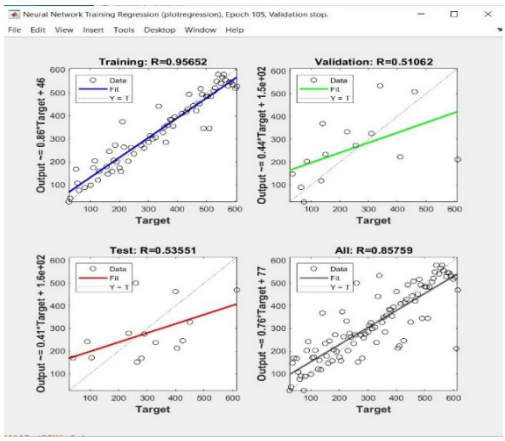

(c)

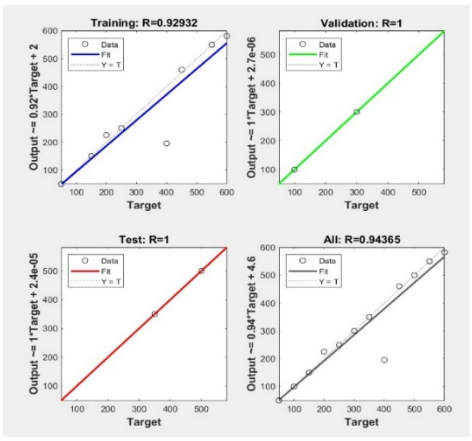

(d)

Fig. 10 Performance of Developed ANN Model; (a) Regression curve for cluster 1; (b) Regression curve for cluster 2; (c) Regression curve for cluster 3; (d) Regression curve for cluster 4

An actual size rail track has been procured from Indian Railways, for monitoring purposes using the AE technique. AE source localisation is done using the developed ANN model for UPV and PLB-induced AE signal on the rail section.

Table 3: localisation of AE sources from WT of the AE signal

Actual Distance (mm)	Localised Distance of PLB (mm)	Localised Distance of UPV (mm)
50	34.15	36.87
100	97.14	97.91
200	198.37	196.46
300	286.44	291.53
400	407.11	389.12
500	491.58	487.39
600	582.17	583.64
700	657.73	649.86
800	756.26	751.69
900	844.97	836.11
1000	901.33	936.75
1100	1054.19	1071.63
1200	1147.51	1136.54

Table 4: Localisation results and Error % at Top Flange

Actual Distance (mm)	Localization results		Error (%)	
	PLB	UPV	PLB	UPV
50	44.149	50.112	13.254	0.223
100	99.254	100.54	0.751	0.537
150	151.413	150.416	0.933	0.277
200	204.179	199.478	2.046	0.262
250	247.576	250.004	0.983	0.002
300	294.255	299.875	1.952	0.042
350	348.642	350.125	0.395	0.033
400	394.756	400.244	1.328	0.053
450	461.399	450.373	2.47	0.083
500	503.126	500.074	0.621	0.015
550	553.855	550.734	0.696	0.115
600	604.53	600.227	0.749	0.038
650	655.652	650.041	0.862	0.006
700	705.921	700.375	0.839	0.054
750	756.676	750.731	0.882	0.097
800	807.331	800.432	0.908	0.054
850	858.022	850.173	0.935	0.02
900	908.745	900.647	0.962	0.072
950	959.425	950.742	0.982	0.078
1000	1010.642	1000.495	1.053	0.049
1050	1060.993	1050.114	1.036	0.011
1100	1111.522	1100.012	1.037	0.001
1150	1162.667	1150.147	1.089	0.013
1200	1212.927	1200.621	1.066	0.052

Table5: Localisation results and Error % at Web

Distance (mm)		Localisation results		Error %	
Actual	**Squared Distance**	**PLB**	**UPV**	**PLB**	**UPV**
50	86.023	86.447	86.230	0.490	0.240
100	122.066	122.456	122.057	0.319	0.007
150	165.529	164.547	165.522	0.597	0.005
200	211.896	214.266	211.810	1.106	0.008
250	259.615	258.021	259.636	0.618	0.008
300	308.058	308.192	308.055	0.043	0.001
350	356.931	355.153	356.925	0.501	0.002
400	406.079	397.164	406.075	2.245	0.001
450	455.412	442.559	455.455	2.904	0.003
500	504.876	487.954	504.845	3.468	0.006
550	554.437	533.349	554.218	3.954	0.039
600	604.070	578.744	604.086	4.376	0.003
650	653.758	624.139	653.165	4.746	0.091
700	703.491	669.535	703.563	5.072	0.010
750	753.260	714.930	753.179	5.361	0.011
800	803.057	760.325	803.045	5.620	0.001
850	852.877	805.720	852.350	5.853	0.062
900	902.718	851.115	902.681	6.063	0.011
950	952.575	896.510	952.156	6.254	0.044
1000	1002.447	941.905	1003.015	6.428	0.057
1050	1052.331	987.301	1053.276	6.587	0.090
1100	1102.225	1032.696	1103.594	6.733	0.120
1150	1152.128	1078.091	1154.566	6.867	0.211
1200	1202.040	1123.486	1205.564	6.992	0.292

Table 6: Localisation results and Error % at Bottom Flange

Distance (mm)		Localisation results		Error %	
Actual	**Squared Distance**	**PLB**	**UPV**	**PLB**	**UPV**
50	177.200	173.512	177.432	2.126	0.130
100	197.231	198.115	197.240	0.446	0.005
150	226.716	224.017	226.472	1.209	0.112
200	262.488	260.997	262.658	0.571	0.065
250	302.324	300.731	302.556	0.530	0.077
300	344.819	343.418	344.875	0.408	0.016
350	389.102	390.653	389.473	0.397	0.095
400	434.626	434.013	434.615	0.141	0.003
450	481.041	480.984	481.591	0.014	0.100
500	528.110	527.156	528.002	0.181	0.020
550	575.674	574.257	575.615	0.247	0.010
600	623.618	622.774	623.563	0.136	0.009
650	671.863	670.841	671.876	0.152	0.017
700	720.347	719.479	721.564	0.119	0.169
750	769.025	768.115	770.341	0.119	0.171
800	817.863	816.740	817.873	0.137	0.001
850	866.833	876.366	866.228	1.088	0.070
900	915.915	918.991	915.796	0.335	0.013
950	965.091	964.616	965.156	0.049	0.007
1000	1014.347	1013.242	1013.597	0.109	0.074
1050	1063.673	1065.867	1064.593	0.206	0.086
1100	1113.059	1117.493	1113.743	0.397	0.061
1150	1162.497	1061.118	1167.336	9.554	0.414
1200	1211.982	1212.744	1212.559	0.063	0.048

Table 3 is representing the localised distances over the rail section using signal processing approach called WT. It is observed from the **Table 3** that up to 300 mm distance AE sources can be localised perfectly using WT-based localisation approach. Due to close walls of the rail section reflection and mode mixing make the localisation process critical. It is also observed that the AE signal induced by UPV and PLB is giving similar localisation result. The other above-mentioned tables are representing the localisation result for source to sensor distances. Error percentage is calculated for the calculated distances with respect to actual physical source to sensor distances. **Table 4** describes the source to sensor distances and error percentages in calculated distances when the AE signal is generated and recorded at TF .**Fig. 11** shows the graphical representation between error percentages with increasing distance for both PLB and UPV-induced signals. It is evident from the figure that UPV-induced AE signals are causing lower error percentages in localisation than PLB generated AE signals. **Table 5** and **Table 6** describe the percentage error of localisation when AE signals are recorded at Web and BF, respectively. **Fig. 12** and **Fig. 13** are the graphical representation of the localisation results with the squared distances at Web and BF. The error percentages in source localisation for UPV-induced AE signals are relatively lower than PLB generated signals in these segments of the rail section also. Moreover, it can be also observed that UPV-induced signals produce consistent location error percentage range throughout the source-to-sensor distances, whereas PLB signals produce inconsistent error percentages.

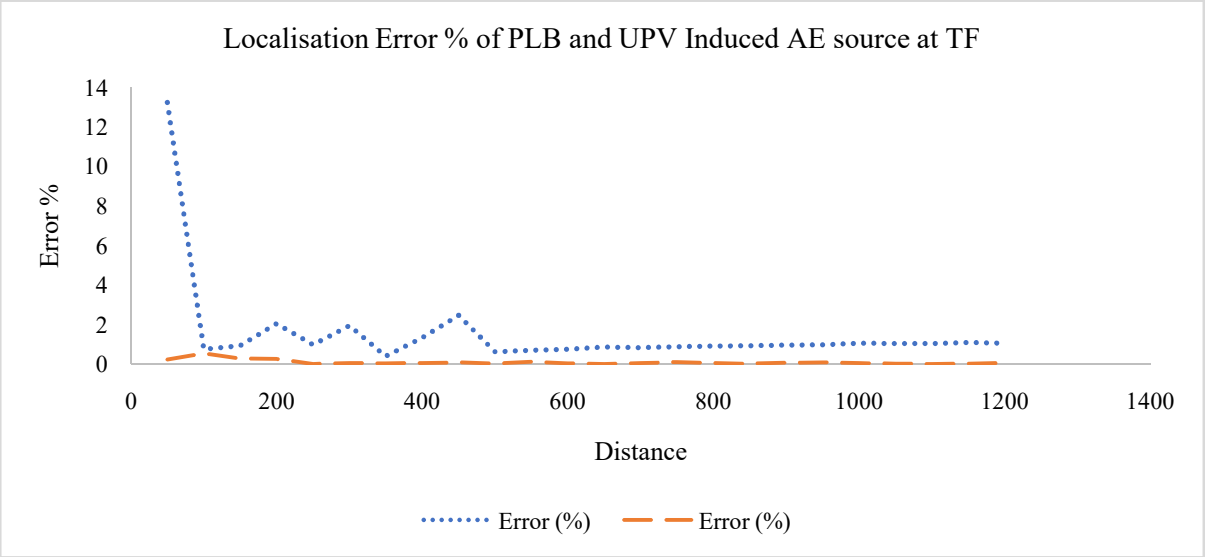

Fig: 11 Error Percentage of Localisation Result with Distance when AE signal Acquired at TF

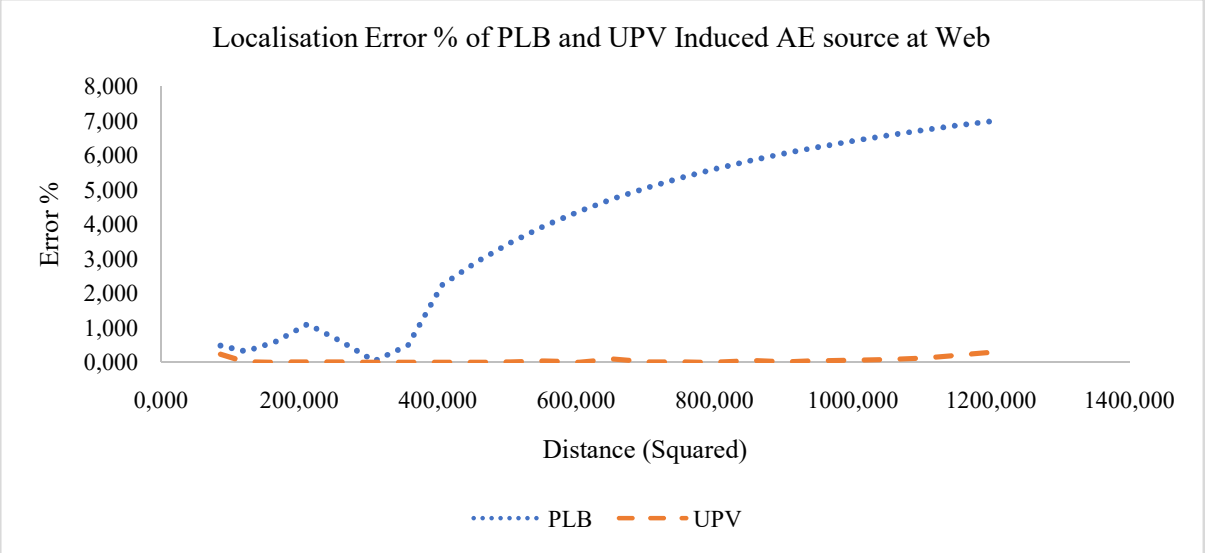

Fig: 12 Error Percentage of Localisation Result with Distance when AE signal Acquired at Web

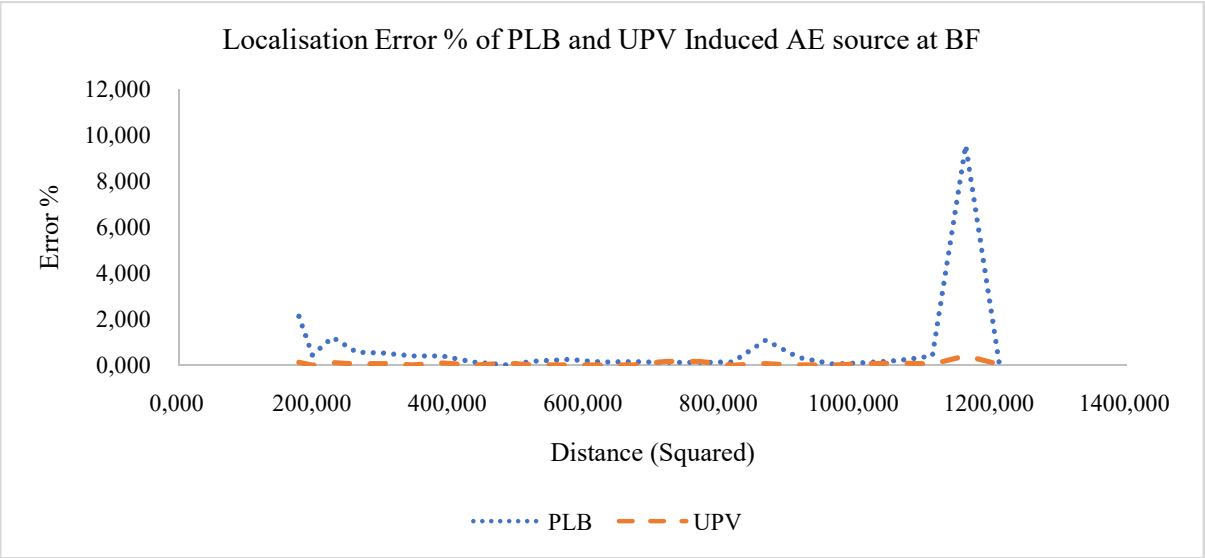

Fig: 13 Error Percentage of Localisation Result with Distance when AE signal Acquired at BF

Conclusion

An experimental study is carried out towards the replacement of the conventional AE source simulation technique, i.e., PLB, with a UPV instrument. It is observed from the WT diagram and the waveform comparison the UPV instrument emits a similar AE signal to PLB. Moreover, ANN is giving more localisation distance of AE source to sensor accurately than WT-based localisation distance. In WT-based localisation, the AE signal need to be accurate every time. Thus, PLB need more expertise to produce similar AE signal by maintaining accurate angle every time. Even with the expertise, due to manual operation, PLB can produce inconsistent AE signals. Generating consistent AE signals is easier for the UPV instrument due to its complete automated operation. Additionally, the UPV instrument can emit ultrasound signals at different frequencies. A developed ANN model is used to localise the AE sourceusing the signals induced by PLB and UPV instruments. It is observed that UPV-induced AE signals produce lower error percentages in source localisation than PLB ones. Moreover, UPV-induced AE signals produce consistent error percentages throughout the source-to-sensor distances for different segments of the rail section. Finally, it can be concluded that the PLB can be replaced with the UPV instrument for laboratory investigations and offline monitoring of rail sections.

Acknowledgement

This study is supported and funded by the Department of Science and Technology (DST)-TSDP, Government of India. The authors are thankful to the Section Engineer (Mr. Deepak Kumar), Assistant Engineer, DGP/E-RLY/Indian Railway for providing the rail section which is used for this study.

Disclosures

Free Access to this article is sponsored by SARL ALPHA CRISTO INDUSTRIAL.

References

1. Kundu, T. (2014). Acoustic source localization. Ultrasonics, 54(1), 25-38.
2. Roy, P., Sengupta, S., Topdar, P., & Datta, A. K. (2023). On the Applicability of Wavelet Transform in Localising Defect in a Small Plate Using AE Technique: An Experimental Study. In International Conference on Advances in Structural Mechanics and Applications (pp. 226-237). Springer, Cham.
3. Sengupta, S., Roy, P., Topdar, P., & Datta, A. K. (2021). Investigation of layered composite plates under acoustic emission using an appropriate finite element model. Canadian Journal of Civil Engineering, 48(12), 1639-1651.
4. Kundu, T., Datta, A. K., Topdar, P., Sengupta S., (2020). An experimental study on optimum placement of ae sensor for localizing damage in the rail section. CRSIDE 2020. 1(1), 1901-1909.
5. Zhang, X., Feng, N., Wang, Y., & Shen, Y. (2014). An analysis of the simulated acoustic emission sources with different propagation distances, types and depths for rail defect detection. Applied Acoustics, 86, 80-88.
6. Hamstad, M.A., O'Gallagher, A. and Gary, J.M., 1999. Modeling of buried monopole and dipole sources of acoustic emission with a finite element technique.
7. Hamstad, M.A. and Gary, J., 2002. A wavelet transform applied to acoustic emission signals: part 2: source location. In Journal of Acoustic Emission.
8. Hamstad, M., O'GALLAGHER, A. and Gary, J., 2002. A wavelet transform applied to acoustic emission. J. Acoust. Emiss, 20, pp.39-61.
9. Anastasopoulos, A., Bollas, K., Papasalouros, D. and Kourousis, D., 2010, September. Acoustic emission on-line inspection of rail wheels. In Proc. 29th Eur. Conf. Acoust. Emission Testing (pp. 1-8).

10. Kuang, K.S.C., Li, D. and Koh, C.G., 2016. Acoustic emission source location and noise cancellation for crack detection in rail head. Smart Struct. Syst, 18(5), pp.1063-1085.
11. Murav'ev, V. V., Murav'ev, M. V., &Murav'ev, T. V. (2008). The possibilities of acoustic emission testing of rails during exploitation. Russian Journal of Nondestructive Testing, 44(1), 33-40.
12. Bassim, M.N., Lawrence, S.S. and Liu, C.D., 1994. Detection of the onset of fatigue crack growth in rail steels using acoustic emission. Engineering Fracture Mechanics, 47(2), pp.207-214.
13. Bruzelius, K. and Mba, D., 2004. An initial investigation on the potential applicability of Acoustic Emission to rail track fault detection. Ndt& E International, 37(7), pp.507-516.
14. Li, D., Kuang, K.S.C. and Koh, C.G., 2018. Rail crack monitoring based on Tsallissynchrosqueezed wavelet entropy of acoustic emission signals: A field study. Structural Health Monitoring, 17(6), pp.1410-1424.